MOLECULAR ORBITAL STUDY OF THE FRAGMENTATION MECHANISM ON 5-HYDROXYTETRAZOLE

Kunio Waki[a], Teruo kurihara[b*], Shigeo Arai[b], and Yoshitada Koyama[b]
a Department of Applied Chemistry, Faculty of Engineering,
Toyo University, Kawagoe-shi, Saitama 350, Japan
b Department of Chemistry, Faculty of Science, Josai University,
Sakado-shi, Saitama 350-02, Japan

Abstract : The tautomerism of 5-hydroxytetrazole is discussed on the basis of its fragmentation patterns and molecular orbital calculations by MNDO and PM3 methods. The calculated results of the fully optimized structures of 5-hydroxytetrazole and radical cations indicate that, in the gaseous phase, the enol form is energetically preferred form.

Introduction

In a previous paper (1), the present first author examined the thermal decomposition of 5-hydroxytetrazole **4** by use of sealed-cell, as a concerning research series about the availability of gas-generating chemicals. The main products were N_2 and urazole, and included a small amount of a resinoid in the condensed phase. Small amounts of CO, CO_2, carbamoylazide, and trace amounts of NH_3 and H_2O were also found in the gaseous and sublimated products. According to the theory, tetrazole and 5-substituted tetrazoles are known to exist in either two or four tautomeric forms. The thermal decomposition, mass spectrometric fragmentation, and molecular orbital calculation of tetrazole and its derivatives have been examined in numerous studies (2-9). Razynska et al. (2) reported on the tautomerism of tetrazole **1**, 5-methyltetrazole **2**, and associated isotopically substituted derivatives in the gaseous phase. It was demonstrated from the mass-spectrometric results, supported by semiempirical calculation (CNDO/2) and then only the 2H tautomer occurred in the gaseous phase. From the results of ab-initio calculation, Mazurek and Osman (3) reported that the preference of the 2H tautomer in gaseous phase, taken together with the suggested fragmentation from structure optimization, explained the observed fragmentation in the mass-spectra of **1** and **2**. According to the mass-spectrum analysis of **1**, **2**, and 5-aminotetrazole **3**, the most abundant ions are formed owing to the loss of N_2 fragments (2-9). On the other hand, a characteristic feature of the high-resolution mass-spectrum of 5-hydroxytetrazole **4** showed at m/z 86 (M^+), 69 (M^+-OH), 44 (CH_2NO), and 43 (HN_3 or CHNO) (1). Compound **4** was found to have no fragment ion peak in its mass-spectrum owing to the loss of N_2. Here, the investigations were extended to include the fragmentation of the tetrazole ring in **4**, along with the revision of several earlier reported results. To advance the further investigation of the properties of tetrazole tautomers, the full geometrical optimizations of the molecules were carried out by MNDO and PM3 methods.

Theoretical Procedure

The molecular orbital calculations by MNDO and PM3 methods were performed with the application of MOPAC program (Version 6.01) (10). The geometries of the neutral species 1-4, and their radical cations 1'-4' were optimized with respect to all geometrical parameters using Broyden-Fletcher-Goldfrab-Shanno algorithm incorporated in the program. The transition states were determined either by the normal reaction coordinate method, or with the use of NLLSQ algorithm, refined by minimizing the energy gradient norm. Force constant calculations were conducted on the transitional state geometry to verify the existence of only one negative eigenvalue.

Results and Discussion

Tetrazole 1 can exist in two tautomeric forms, while 5-substituted tetrazoles 2-4 are known to exist in each four tautomeric form (2-9) (Fig. 1). First, the geometries of 1-4 were optimized. Table I

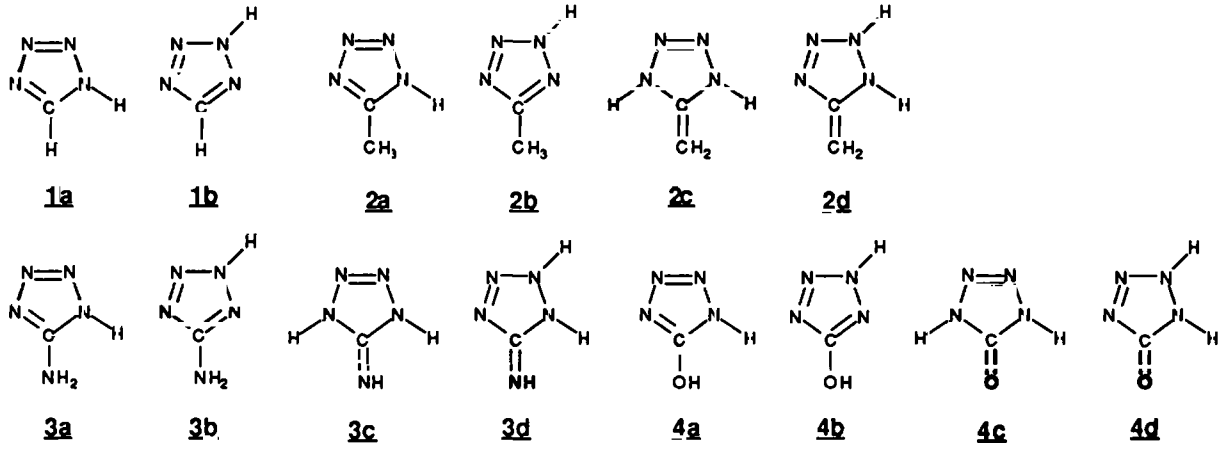

Figure 1: Illustrations of tautomeric forms of 1-4

Table I : Heat of formation ΔH_f (kJmol^{-1}) on tautomers 1-4 by MNDO and PM3 methods

	ΔH_f			ΔH_f	
	MNDO	PM3		MNDO	PM3
1 a	225.279	360.870	3 a	214.681	350.778
1 b	243.166	369.953	3 b	232.170	358.393
			3 c	277.567	392.041
			3 d	319.469	432.797
2 a	177.213	316.992	4 a	16.468	173.945
2 b	194.477	328.674	4 b	39.079	192.301
2 c	268.592	378.903	4 c	40.238	150.252
2 d	313.649	429.747	4 d	91.701	198.937

summarizes the values of the heat of formation (ΔH_f) of 1a-1b, 2a-2d, 3a-3d, and 4a-4d obtained by MNDO and PM3 methods. The 1H tautomer 1a is preferred over 2H tautomer 1b by 17.89 and 9.08kJmol^{-1}, according to MNDO and PM3 methods, respectively. On the other hand, the results of the 6-31G**, by Mazurek and Osman (3) reverse the evaluation of energy compared with the present MNDO and PM3 calculations. The difference in the optimized bond lengths does not exceed 0.03Å for tautomers 1-4. The largest change in the optimized angles was about 3.0° for tautomers of 1-4. The microwave estimate of the dipole moment of 1b was 2.19D (11) and the present MNDO and PM3 calculations were 1.89D and 2.34D, respectively. Krugh and Gold (11) obtained a dipole moment 5.30D for the 1H tautomer 1a. The present MNDO and PM3 calculations gave dipole moments for 1a of 5.09D and 5.41D, respectively. Two dipole moments were also supported by Krugh and Gold (11). The positions of the lone-pair electron on the nitrogen atom in 1a and 1b are located at N(2) and N(4) atom, respectively. If it is assumed that the lone-pair electron on N(2) or N(4) atom is ionized by electronic impact, then N_2 fragment is expected. For 2a and 2d tautomers, the position of the lone-pair electron is located at N(4) atom. For 4a and 4b tautomers, the positions of the lone-pair electron are located at N(3) and N(4) atom, respectively. Under such circumstances, the preferred fragmentation of tautomers 2-4 could yield N_2 fragments. Therefore, the results expected for tautomer 4 did not agree with the observed mass-spectra of 4. Second, the geometries of the radical cations 1'-4' were optimized.

Table II : Heat of formation ΔH_f (kJmol^{-1}) on the radical cations 1'- 4' by MNDO and PM3 methods

	ΔH_f			ΔH_f	
	MNDO	PM3		MNDO	PM3
1a'	1227.167	1376.440	3a'	1116.069	1211.795
1b'	1254.313	1343.336	3b'	1100.584	1174.679
			3c'	1152.960	1226.422
			3d'	1226.414	1297.103
2a'	1173.093	1300.546	4a'	994.784	1137.843
2b'	1177.457	1265.405	4b'	983.011	1115.392
2c'	1045.255	1158.211	4c'	992.449	1072.920
2d'	1116.806	1226.473	4d'	1042.071	1107.287

Table II summarizes the values of ΔH_f for the radical cations (1a'-1b', 2a'-2d', 3a'-3d', and 4a'-4d') obtained by MNDO and PM3 methods. The relevant geometrical parameters for PM3 method of the tautomers are summarized in Table III. From the date listed in Table II, 1H tautomer 1a' is preferred over 2H tautomer 1b' by 27.15kJmol^{-1} according to MNDO method, but 1b' is preferred over 1a' by 33.10kJmol^{-1} using PM3 method. Mazurek and Osman (3) reported that on the radical 1b'. the N(3)-N(2) bond length increased beyond 2Å during optimization at the UHF/3-21G level. In the UHF/PM3 optimized structures, the N(3)-N(2) bond lengths of 1b', 2b', and 4b' were calculated as 1.783Å, 1.749Å, and 1.673Å, respectively, in agreement with the results of Mazurek

and Osman. Thus, the transition states and energies of activation (Ea) for the radical cations 1'-4' were determined by UHF/PM3 method. The ΔH_f values of 4a'-4d' were calculated by PM3 method as 1137.8, 1115.4, 1072.9, and 1107.3kJmol^{-1}, respectively. Compound 4c' had the most stable

Table III : Optimized geometries of radical cations 1'-4' on calculation by PM3 method

Structural parameters	Tetrazole (1)		5-Methyltetrazole (2)			
	1 a '	1 b '	2 a '	2 b '	2 c '	2 d '
	Bond lengths (Å)		Bond lengths (Å)			
N1N2	1.648	1.252	1.302	1.251	1.352	1.379
N2N3	1.200	1.783	1.408	1.749	1.268	1.386
N3N4	1.403	1.175	1.238	1.180	1.351	1.246
N4C5	1.404	1.463	1.452	1.473	1.402	1.434
C5N1	1.329	1.401	1.413	1.409	1.402	1.413
	Bond angles (degrees)		Bond angles (degrees)			
N1N2N3	104.42	104.31	108.34	105.14	109.43	108.06
N2N3N4	113.65	99.69	109.50	100.89	109.64	109.91
N3N4C5	109.87	117.64	110.46	116.43	109.67	111.29
N4C5N1	106.68	106.22	102.35	105.86	101.51	103.97
C5N1N2	105.18	112.14	109.36	111.67	109.75	106.60

Structural parameters	5-Aminotetrazole (3)				5-Hydroxytetrazole (4)			
	3 a '	3 b '	3 c '	3 d '	4 a '	4 b '	4 c '	4 d '
	Bond lengths (Å)				Bond lengths (Å)			
N1N2	1.316	1.302	1.337	1.344	1.315	1.270	1.308	1.317
N2N3	1.331	1.395	1.280	1.453	1.390	1.673	1.310	1.668
N3N4	1.270	1.251	1.335	1.223	1.240	1.194	1.307	1.182
N4C5	1.426	1.436	1.420	1.467	1.466	1.478	1.478	1.518
C5N1	1.416	1.394	1.422	1.473	1.410	1.402	1.478	1.514
	Bond angles (degrees)				Bond angles (degrees)			
N1N2N3	109.44	110.66	109.86	108.73	109.26	106.68	110.91	106.96
N2N3N4	110.73	108.72	110.17	109.41	110.69	104.14	111.11	105.51
N3N4C5	109.15	108.62	109.40	112.33	108.60	112.22	109.48	115.83
N4C5N1	102.67	105.76	101.12	102.63	103.80	107.97	98.94	102.95
C5N1N2	108.02	106.25	109.44	106.83	107.66	109.00	109.56	108.62

cation among these tautomers. The total bicentre energies and properties of the transitional states of the radical cations 4a'-4d' are listed in Table IV. An analysis of the values of the bicentre energy $E_{\alpha\beta}$ of tautomer 4c' shows that N(4)-C(5) or C(5)-N(1) bonds should be easily broken. To determine exactly what happens during and after the N(4)-C(5) bond or C(5)-N(1) bond fission, the reaction coordinate calculations were performed by stretching the N(4)-C(5) or C(5)-N(1) bonds in the radical cation 4c'. The reaction pathway was calculated by the appropriate reaction coordinate N(4)-C(5) bond lengths. The geometry of the molecule when the bond is stretched to 2.247Å is suggestive of a transitional state, since there is only one negative

eigenvalue of 295.6cm^{-1}. From the results of normal coordination analysis, the most probable fragmentation of **4c'** would yield N_3H or NCOH fragments (Figure 2A). The activation energy for this process was determined as 86.73kJmol^{-1}. The optimization of the transitional state of radical cation **4c'** was accomplished by stretching the C(5)-N(1) bond as the reaction coordinate

Table IV : Calculated properties of the transitional states for the bond cleavage of **4a'**-**4d'**

			TS[a]			
		Eαβ[b]	Reaction coordinate	ΔHf[c]	ν[d]	Ea[e]
4a'	N1N2	-16.506				
	N2N3	-13.032		not determined		
	N3N4	-20.260				
	N4C5	-13.311	2.145	1266.75	503	170.71
	C5N1	-15.907				
4b'	N1N2	-18.803				
	N2N3	-7.178	2.104	1135.45	477	19.08
	N3N4	-23.335				
	N4C5	-12.602				
	C5N1	-16.011				
4c'	N1N2	-16.764				
	N2N3	-16.345				
	N3N4	-16.780				
	N4C5	-13.111	2.247	1157.34	296	86.73
	C5N1	-13.115	2.247	1165.70	297	86.65
4d'	N1N2	-16.992				
	N2N3	-7.140	1.995	1114.87	292	7.28
	N3N4	-24.047				
	N4C5	-11.916				
	C5N1	-11.126				

a) Transition state. b) Bicentre energy in eV. c) Heat of formation in kJmol^{-1}.
d) Imaginary mode in cm^{-1}. e) Energy of activation in kJmol^{-1}.

with the application of NLLSQ algorithm. When the C(5)-N(1) bond is stretched to 2.247Å, the geometry of the molecule suggests a transitional state, since there is only one negative eigen value of 296.8 cm^{-1}. In Figure 2B, the most probable fragmentation process of **4c'** would yield N_2H or CON_2H fragments. The activation energy calculated for this process was 86.65kJmol^{-1} (Table IV). The analysis of the $E_{\alpha\beta}$ values of **4d'** shows that N(2)-N(3) bond should be readily broken in this radical. The transitional state was calculated by N(2)-N(3) bond length as the reaction coordinate. In Figure 2C, the preferred fragmentation of **4d'** could yield N_2 or CON_2H_2 fragments. The activation energy for the process was 7.28kJmol^{-1} (Table IV). For the radical cation **4b'**, from the results of the imaginary mode (Figure 2D) with a eigenvalue of 477cm^{-1}, the most probable fragmentation of **4b'** could yield N_3H or NCOH fragments.

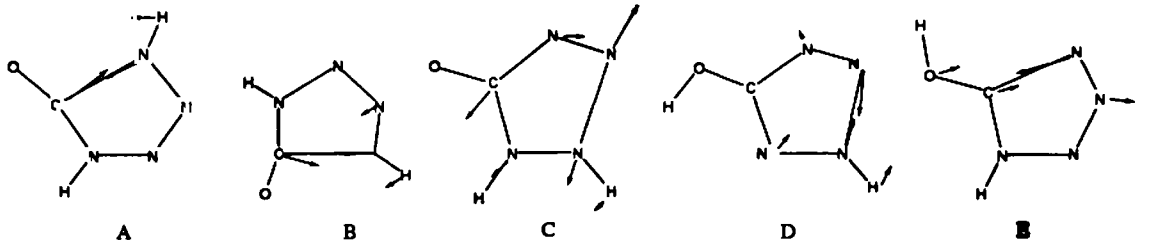

Figure 2 : Illustrations of vectors of imaginary modes

The $E_{\alpha\beta}$ values for the radical cation **4a'** showed that N(2)-N(3) or N(4)-C(5) bonds should be more readily broken. When the reaction pathway was calculated by N(2)-N(3) bond length as the reaction coordinate, the transitional state could not be determined. Because two negative eigenvalues were found. When the N(4)-C(5) bond of **4a'** is stretched to 2.145Å, the results are suggestive of a transitional state with one negative eigenvalue of 503.0cm^{-1}. In Figure 2E, the preferred fragmentation of **4a'** could yield N_3H or,NCOH fragments. While the radical **4c'** had the smallest ΔH_f value, the value of Ea determined for **4c'** was larger than those of **4b'** and **4d'**. Therefore, the fragmentation mechanism from **4a'** could not explain the observed fragmentation in the mass-spectra of **4**. The results of the present UHF/PM3 level calculations suggest that the preferred fragmentation of **4'** could yield fragments of N_2 or $COHN_2H_2$ from **4d'** when comparing with the Ea values. The difference between the Ea values in the transitional states of **4b'** and **4d'** was small. By PM3 method, it is found that **4d'** was slightly preferred over **4b'** by 8.11kJmol^{-1} (Table II). By MNDO method, however, **4b'** was preferred over **4d'** by 59.06kJmol^{-1}. From the above results, the most preferred fragmentation of the radical cation **4'** could yield N_3H or CHNO fragments, because the most susceptible bond for stretching is the N(2)-N(3) in radical **4b'**. The total bicentre energies of **1'**, **2'**, and **3'** are listed n Table V. The transitional states and energies

Table V : Total bicentre energy $E_{\alpha\beta}$ (eV) of the radical cations **1'**-**3'** by UHF/PM3 method

	Tetrazole		5-Methyltetrazole				5-Aminotetrazole			
$E_{\alpha\beta}$	**1a'**	**1b'**	**2a'**	**2b'**	**2c'**	**2d'**	**3a'**	**3b'**	**3c'**	**3d'**
N1N2	-7.63	-19.58	-16.97	-19.71	-14.79	-14.50	-16.47	-17.50	-15.43	-15.86
N2N3	-22.54	-4.88	-12.41	-5.53	-18.61	-13.22	-15.24	-13.24	-17.90	-11.27
N3N4	-12.12	-24.55	-20.39	-24.26	-14.81	-19.88	-18.42	-19.82	-15.52	-21.31
N4C5	-15.80	-12.89	-13.99	-12.78	-17.17	-14.86	-15.26	-14.88	-16.58	-13.70
C5N1	-20.04	-15.85	-16.08	-15.66	-17.18	-16.29	-17.19	-16.43	-16.20	-13.53

of activation of **1a'** and **1b'** were carried out in a manner that stated above. The values of the $E_{\alpha\beta}$ for **1a'** and **1b'** revealed that the respective bonds N(1)-N(2) and N(2))-N(3) should be most readily broken. The transition state of the radical **1a'** was calculated by N(1)-N(2) bond as the reaction coordinate. The geometry of the molecule when the bond is stretched to 2.053Å suggests

a transitional state. From the results of the imaginary mode (Figure 3A), the most probable fragmentation of **1a'** would yield a N_2H fragment. The activation energy for this process was calculated 26.53kJmol^{-1}. The geometry of the molecule in **1b'** when the bond is stretched 2.096Å

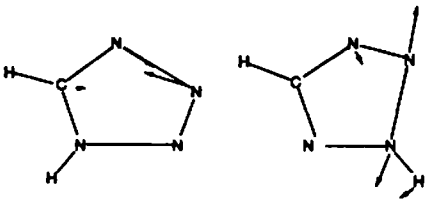

A B

Figure 3 : Illustrations of vectors of imaginary modes

suggests a transitional state with one negative eigenvalue of 459.60cm^{-1}. The most probable fragmentation of **1b'** might yield a N_2 fragment (Figure 3B). The activation energy for this process is 10.67kJmol^{-1}. Consequently, for the radical cation **1'**, comparing with the Ea values, the most abundant ions are formed due to the loss of N_2 fragments. The present UHF/PM3 level calculations reasonably could explain the preferential bond breaking observed in the mass spectrum of tetrazole **1**. For the radical cation **2b'**, when N(2)-N(3) bond was stretched to 1.839Å, only one negative eigenvalue of 469.8cm^{-1} was found. From a vector analysis of 469.8cm^{-1}, the most probable fragmentation of **2b'** might yield N_2 or, CH_3CN_2H fragments.

Acknowledgments

The authors are grateful to Dr. Noboru Motohashi, Meiji College of Pharmacy, Japan, for reviewing the draft and making helpful comments.

References

1. K. Waki and T. Yamashita, Kogyo Kayaku. (in Japanese). **53**, 238 (1992)
2. A. Razynska, A. Tempczyk, E. Malinski, J. Szafranek, Z. Grzonka and P. Hermann, J. Chem. Soc. Perkin Trans II, 379 (1983)
3. A. P. Mazurek and R. Osman, J. Phys. Chem. **89**, 460 (1985)
4. I. Jano, J. Phys. Chem. **95**, 7694 (1991)
5. A. I. Lesnikovich, S. V. Levchik, A. I. Balabanovich, O. A. Ivashkevich and P. N. Gaponik, Thermochimi. Acta. 200. 427 (1992)
6. S. V. Levchik, O. A. Ivashkevich, A. I. Balabanovich, A. I. Lesnikovich, P. N. Gaponik and L. Costa, Thermochimi. Acta. 207. 115 (1992)

7. A. I. Lesnikovich, O. A. Ivashkevich, V. A. Lyutsko, G. V. Printsev, K. K. Kovalenko, P. N. Gaponik and S. V. Levchik, Thermochimi. Acta. **145**. 195 (1989)

8. S. V. Vyazovkin, A. I. Lesnikovich and V. A. Lyutsko, Thermochimi. Acta. **165**. 17 (1990)

9. A. I. Lesnikovich, O. A. Ivashkevich, G. V. Printsev, P. N. Gaponik and S. V. Levchik, Thermochimi. Acta. **171**. 207 (1990)

10. MOPAC ver. 6.00, J. J. P. Stewart, QCPE Bull. **9**, 10 (1989) Revised as ver 6.03 by Yoshihisa Inoue, JCPE Newslett. **4**, 60 (1992)

11. W. D. Krugh and L. P. Gold, J. Mol. Spectrosc. **49**, 423 (1974)

Received April 9, 1995